Physics Journal
Vol. 1, No. 3, 2015, pp. 355-366
http://www.aiscience.org/journal/pj

Vane Structure for the Protection of TC-128 Steel Plate Against High Power Impact

Liguang Cai, Ahmed Al-Ostaz, Xiaobing Li*, Cole Fowler, Hunain Alkhateb, Alexander H.-D. Cheng

Department of Civil Engineering, University of Mississippi, University, USA

Abstract

Increasing the ballistic resistance of the steel railcar tank for carrying toxic liquids is of great significance in terms of preventing liquid leakage. In this paper, three-dimensional numerical simulations have been conducted to study the ballistic performance of railcar tank steel (TC-128) plate under normal and oblique impact. The finite element analysis results in terms of the ballistic limit of TC-128 steel plate are consistent with ballistic limit test results with average error of 8%. Both experimental and numerical simulation results show that the ballistic limit of TC-128 steel plate increased with increasing impact obliquity. A vane structure was proposed to deflect the projectile. As a result, the enhanced impact obliquity increased the ballistic limit of TC-128 steel plate. Two materials, steel 1006 and aluminum were used for the vane structure, respectively. The ballistic limit of the vane-target structure was improved with vane structure obliquity and thickness. At the same vane structure obliquity and thickness, the steel 1006 vane structure is more effective in protecting the TC-128 steel plate than the aluminum vane structure due to higher strength. However, with the same thickness, the "Vane Isolated Performance" (VIP) of the aluminum vane structure is higher than the steel 1006 vane structure because of the lower areal density of aluminum. The analysis was also extended to a double layer aluminum vane structure. The double layer aluminum vane structure could provide better ballistic performance than the single layer aluminum vane structure with the same areal density. Therefore, vane structure obliquity, strength, areal density and distribution density are four most import parameters for vane structure to improve the ballistic limit of TC-128 steel plate. All the simulations were performed in ANSYS AUTODYN finite element code.

Keywords

V-50, Oblique Impact, Vane Structure, Ansys Autodyn

Received: September 14, 2015 / Accepted: December 18, 2015 / Published online: January 5, 2016

1. Introduction

TC-128 steel is a standard material that has been widely used in rail car tank for carrying toxic liquids such as chlorine [1]. However, the release of the toxic liquids from the holes in the tanks, caused by high power impact, is very harmful to the environment and even leads to deadly health risks for humans [2, 3]. Therefore, increasing the ballistic resistance of the tank is of great significance in terms of preventing liquid leakage. Generally, two methods can be used to increase the ballistic limit: using lightweight materials that have super high energy absorption ability as a protection layer and simply increasing impact obliquity [4, 5].

Glass transition temperature is a critical parameter that can contribute to energy absorption. When the glass transition temperature is close to but less than the test temperature, the lightweight materials, such as rubber and polyurea, can transition from the rubbery state to glassy state

* Corresponding author
E-mail address: LXB22@yahoo.com (Xiaobing Li)

accompanied by substantial energy dissipation [6, 7]. Roland [8] found that the elastomer coating can significantly increase the ballistic limit over that of bare high hardness steel (HHS), especially for those elastomers with high and/or broad glass transitions. Grujicic [9] observed a glassy-state with viscous type energy-dissipation for polyurea when the glass transition temperature was slightly lower than the test temperature.

Some oblique impact tests revealed that the ballistic limit increased with increasing impact obliquity. Sadanandan [5] studied the oblique impacts of Swedish FFV armor piercing and U.K. ball ammunition on aluminum and steel plate, and found that ballistic limit increased with impact obliquity, which was due to the increasing energy absorbed by target plate with increasing obliquity [10]. Iqba [11] used ABAQUS to simulate the ballistic resistance of weldox 460 E steel targets subjected to impact by a projectile with a conical nose at different impact obliquities. They found that the ballistic limit of target plates was almost the same from 0 to 30º obliquity but was increased significantly after that. Børvik [12] studied AA6082-T4 aluminum plates under normal and oblique impact by soft NATO ball and hard APM2 bullet. The velocity drop during perforation was almost constant up to 30º then increased for APM2 bullet, whereas a gradual increase in velocity drop with increasing obliquity was observed for NATO ball bullet. For both bullets, the critical oblique angle was less than 60º. More recently, the mechanism of higher impact obliquities result in higher ballistic limit of a structure has been investigated. Baluch [13] studied the oblique impacts of aluminum projectile on an Al6061-T6 spacecraft inner wall. It was found that the damage area and energy absorption of impacted Al6061-T6 specimen increased with increasing impact obliquities. This study agrees well with Roslan's work of oblique impact on kenaf-reinforced composite plate [14]. They found that the raised oblique impact angle added the time of collision which contributed to higher energy absorption response. The larger damage area with higher oblique impact angle was also found in their study. Consequently, the higher impact angle caused larger damage area and higher energy absorption of the target structure after impact, which is the mechanism for the increase of ballistic limit.

In this paper, a vane-target structure is designed to protect TC-128 steel plate, which is shown in figure 1. The vane structure can deflect the projectile when it impacts the vane structure and then impacts the TC-128 steel plate at a certain angle, which can increase the ballistic limit of the TC-128 steel plate. Similar investigation of this type of steel and structure has not been found in publications.

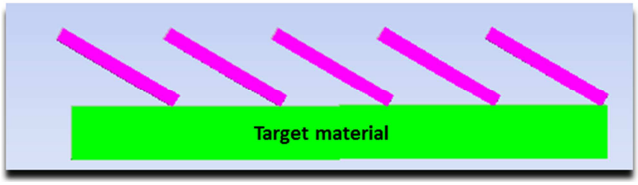

Fig. 1. Schematic illustration of vane-target structure.

A series of 3-D finite element models were developed to study the ballistic limits of TC-128 steel plates at different impact obliquities and the simulation results in terms of ballistic limit were compared with ballistic limit test results. Finite element analysis was also performed to study the ballistic limit of the vane-target structure. The effectiveness of vane structures in protecting the TC-128 steel plates is investigated.

2. Computational Model Verification

2.1. Ballistic Limit Test

2.1.1. Ballistic Limit Test Description

The ballistic limit test was performed at H.P. White Ballistic Laboratory in Stress, MD. During the test, a standard 0.50 caliber M33 ball was shot into the plates which were mounted on a rigid support structure. The parameters of the 0.50 caliber M33 ball round are tabulated in table 1. The 19.05 mm thick TC-128 steel target plates were secured to a floor-mounted heavy steel rack 7.6 m from the test barrel. The plates were secured to the rack by C-clamps. The rack had the capability to rotate in order to provide oblique angles between 0-60º. During the test, impact angles ranged from 0º to 45º in steps of 15º. A laser leveling device was used to align each shot. Two photoelectric infrared screens placed three and six meters forward from the barrel were used in conjunction with a chronograph in order to calculate the average velocity of the projectiles, as shown in figure 2. The velocities were manipulated by increasing or decreasing the amount of propellant used in each cartridge.

A 0.50 mm thick sheet of 2024-T3 aluminum was used as a witness plate to determine partial or complete penetration. If the witness aluminum plate is perforated in conjunction with the target plate, it is considered as complete penetration. Other cases, including projectiles stuck in the target plates, are considered as partial penetration. The range of error can be calculated by the difference between the highest partial and lowest complete penetrations. The ballistic limit value is very accurate if the range of error is less than 15 m/s.

Table 1. Parameters of 0.50 caliber M33 ball round.

Diameter (mm)	Length (mm)	Projectile weight (g)	Velocity (m/s)
12.7	138.4	42.96	914

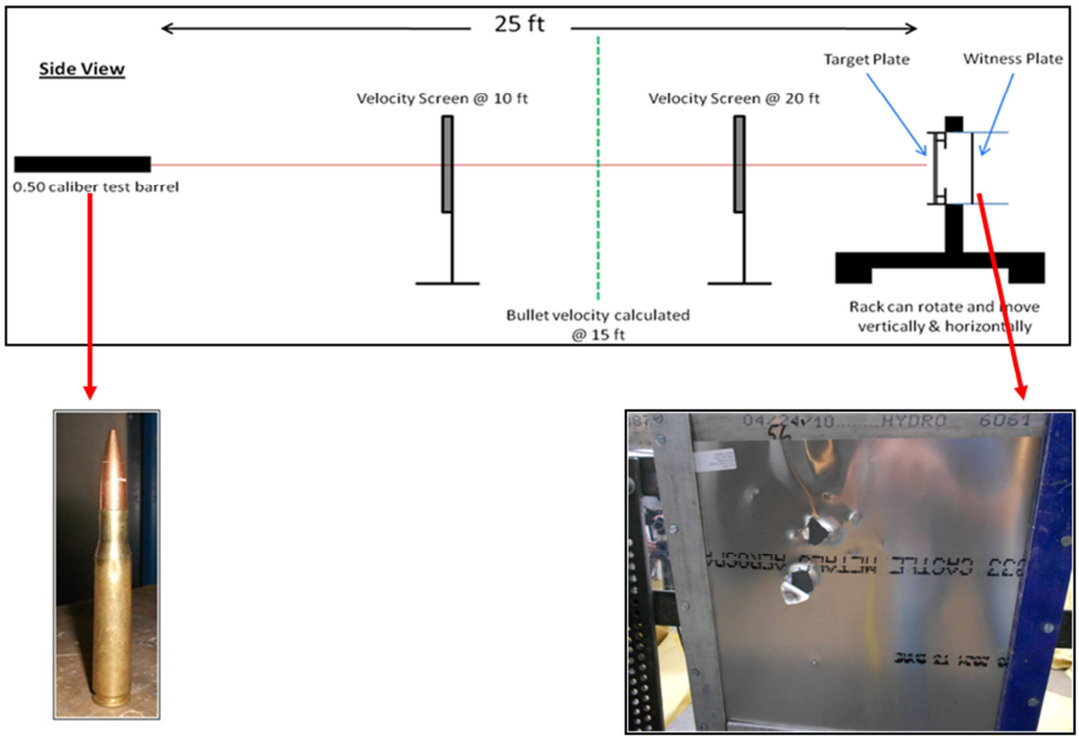

Fig. 2. Experimental setup of the ballistic limit test.

2.1.2. Ballistic Limit Test Results

The experimental results are presented in table 2. For 30º obliquity impact, the ballistic limit value was not accurate because the range of error was 41.1 m/s. For 45º obliquity impact, no ballistic limit value was obtained because the maximum velocity of 1015.9 m/s used in the experiment did not fully perforate the target plate. Therefore, the ballistic limit of steel plate under 45º obliquity impact was higher than 1015.9 m/s. The TC-128 plates under different impact obliquities after the impact are shown in figure 3. The impact craters left in the steel platess increased with increasing impact obliquities, which result in a higher ballistic limit under higher impact obliquity.

Table 2. Ballistic limit test results for TC-128 steel plate at different impact obliquities.

Obliquity of impact (degree)	Shot	Velocity (m/s)	Result	Include	V50 (m/s)	Range (m/s)
0	1	927.5	P	N	971.1	8.8
	2	928.1	P	N		
	3	NR	C	N		
	4	970.8	C	Y		
	5	967.4	P	Y		
	6	976.3	C	Y		
	7	969.6	P	Y		
15	1	980.8	P	Y	985.7	9.8
	2	997.9	C	N		
	3	990.6	C	Y		
30	1	NR	C	N	998.8	41.1
	2	998.8	C	Y		
	3	957.7	P	Y		
45	1	994.3	P	N	NR	
	2	1015.9	P	N		

V-50: ballistic limit, the average velocity at which bullets penetrate the armor equipment in 50% of the shots; P: partial penetration; C: complete penetration; Y: included for V-50 calculation; N: not included for V-50 calculation, NR: no results.

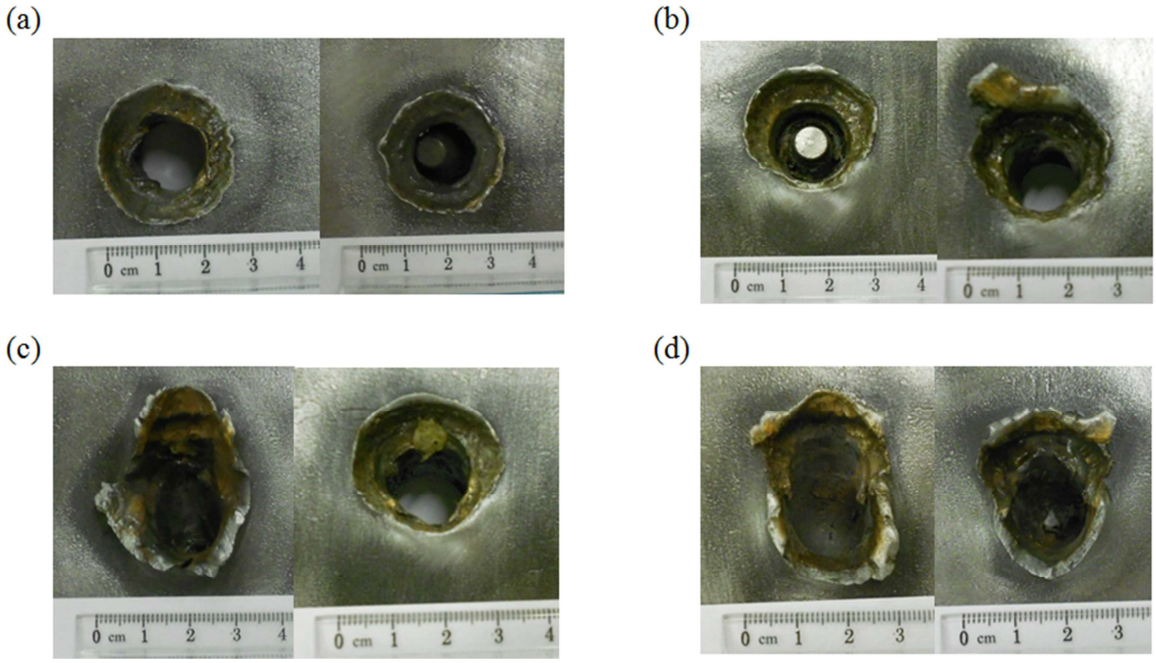

Fig. 3. TC-128 plate after the impact (a) normal impact; (b) 15º obliquity impact; (c) 30º obliquity impact; (d) 45º obliquity impact.

2.2. Finite Element Analysis Model

2.2.1. Material Model

In AUTODYN, the material modeling is composed mainly of three parts, the equation of state (EOS), strength model and failure model. In most cases, the stress tensor can be divided into two parts, hydrostatic pressure corresponding with volume change and stress deviatoric tensor associated with shape change. EOS is the relationship between the hydrostatic pressure, the specific volume and local specific energy. The strength model mainly describes the resistance of a material to shear distortion. The failure model is the criteria of maximum strain or stress that a material can sustain. Normally, following failure, the material cannot sustain shear or tensile stress anymore.

(i) Projectile

The main two components of the projectile are a copper jacket and steel core. During the test, the copper jacket was totally ripped off. This is because the strength of the copper jacket is much lower than that of the TC-128 steel plate. In addition, Børvik et al [15] found that a brass jacket, which has a much higher strength than a copper jacket, has almost no influence on the ballistic limit of steel targets. So, for all the simulations, the steel core was used to represent the whole projectile.

EOS of the steel core is linear and defined as:

$$P = ku \tag{1}$$

Where K is the material bulk modulus, and u is the specific volume.

For the strength model, the material properties of the steel core are uncertain because the required test data are generally not available in the literature. The Rockwell C hardness (HRC) value of the steel core, which is the only known parameter, is equal to 53 and was provided by the H.P White Company. So, the tensile test data of Arne tool steel with an HRC value equal to 53 was used for the steel core [16]. The bilinear hardening strength model is used to fit the experimental data. The expression of the bilinear hardening strength model is,

$$\sigma = \begin{cases} E\varepsilon & \varepsilon \le \varepsilon_0 \\ \sigma_0 + E_t(\varepsilon - \varepsilon_0) & \varepsilon > \varepsilon_0 \end{cases} \tag{2}$$

Where E is the Young's modulus and E_t is the tangent modulus.

The failure model for the projectile was not considered at this stage, but the erosion technique was used to represent the failure of the projectile material. If the effective plastic strain (EPS) in an element reached a value of 1, this element is deleted from further calculation. The model constants for the projectile are reported in table 3.

Table 3. Model constants for the projectile.

Equation of State				**Strength Model**			**Erosion**
ρ(g/cm^3)	K (G pa)	T_0(k)	C_p (J/kg.^{o}k)	G (Gpa)	σ_o (MPa)	E_t(GPa)	EPS
7.75	200	300	477	76.69	1,900	15,000	1

(ii) TC-128 steel plates

The equation of state (EOS) of TC-128 steel also can be described by equation (1), which only needs one parameter. For the strength model, the quasi-static tensile test is performed for TC-128 steel plate at room temperature and a strain rate of 5 x 10^{-4} /s. The engineering stress-strain curve and true stress-strain curve are plotted at figure 4. The Piecewise Model, a modification model to the Johnson-Cook model, was used as the strength model for TC-128 steel plate. For the Johnson-Cook model (JC model), the stress can be express as a function of strain, strain rate and temperature, i.e.:

$$\sigma = \left[A + B\varepsilon_{pl}^{n}\right]\left[1 + Cln\dot{\varepsilon}_{pl}\right]\left[1 - T_{H0}^{m}\right] \quad (3)$$

Where ε_{pl} is the equivalent plastic strain; $\dot{\varepsilon}_{pl}$ is the equivalent plastic strain rate; A, B, and C are material parameters (A is the initial yield stress, B is the hardening constant, and C is the strain rate constant); n and m are respectively the hardening exponent and thermal softening exponent; and $T_{H0} = (T - T_{room})/(T_{melt} - T_{room})$ and is the non-dimensional normalized (homologous) temperature (T_{room} is room temperature while T_{melt} is the melting temperature). All temperatures are given in Kelvin.

For the piecewise model, strain rate hardening and thermal softening parts remain the same as in the JC model while the strain hardening part $\left[A + B\varepsilon_{pl}^{n}\right]$ in the JC model is replaced by a piecewise linear function of yield stress versus effective plastic strain. For the piecewise model built in AUTODYN software, the strain hardening part can be obtained by up to ten EPS and effective stress (ES) data points. For the strain rate constant C and thermal softening exponent m , the parameters of weldox 460 E steel ,which has almost the same yield strength and tensile strength as TC-128 steel, are used here [17].

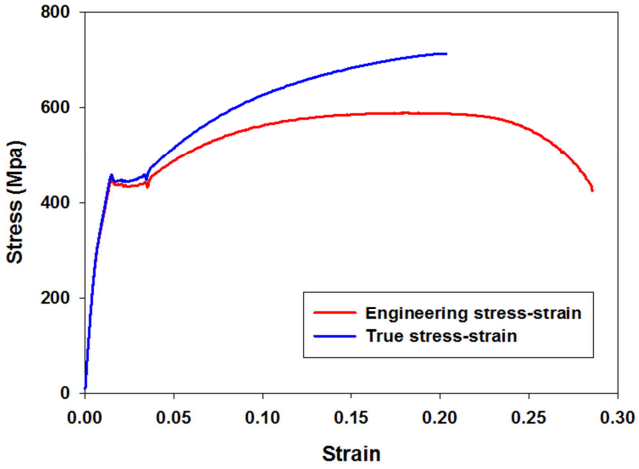

Fig. 4. True and engineering stress-strain curves of TC-128 steel.

The failure model of TC-128 steel is based on the EPS value. When the EPS exceed the 1, element failure occurs. The model constants for TC-128 steel plate are reported in table 4.

Table 4. Model constants for TC-128 steel.

Equation of State				**Erosion**
ρ(g/cm^3)	**K (GPa)**	**T_0(k)**	**C_p (J/kg.^{o}k)**	**EPS**
7.98	181	300	455	1

Strength Model							
G (Gpa)	**σ_o (MPa)**	**EPS 1~6**					
76	455	0.0004	0.0057	0.03	0.1	0.17	0.2

Strength Model									**Failure model**
ES 1~6 (MPa)						**C**	**M**	**T_m(^{o}k)**	**EPS**
448	446	506	646	704	707	0.006	0.893	1800	1

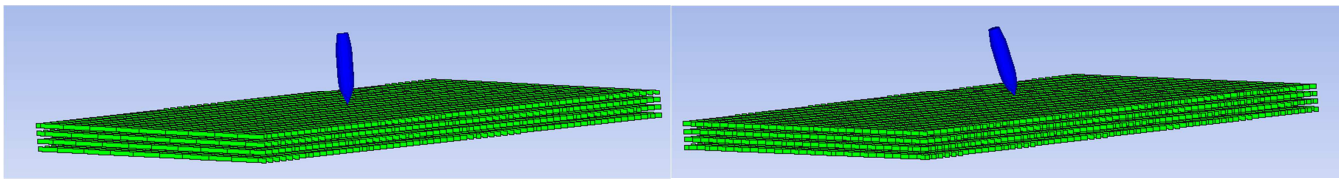

(a) (b)

Fig. 5. Architecture of the model (a) 0 degree (b) 15 degree.

2.2.2. Architecture of the Model

The Lagrange and SPH solver are used for the projectile and target respectively. The total number of elements in the projectile is 3400, and the total number of particles in the targets is 14400. The architecture of the model is shown in figure 5. The impact angle increased from 0º to 15º. The dimension of TC-128 steel plate is 300 mm × 300 mm × 9.05 mm, which are the dimensions of TC-128 steel plate used in the V-50 test.

2.2.3. Verification of the Finite Element Analysis Models

The numerical results of the investigation for ballistic resistance of TC-128 steel plate at different impact obliquity are reported in table 5. For the computational model, the ballistic limit is the average value of the highest partial and lowest complete penetration velocity.

Table 5. Simulation results in terms of ballistic limit for blank TC-128 steel plate at different impact obliquity.

Obliquity (Degree)	Impact velocity (m/s)	Result	Residual velocity (m/s)	V_{50} (m/s)
0	860	P	0	875
	870	P	0	
	880	C	49.3	
15	900	P	0	925
	910	P	0	
	920	P	0	
	930	C	40.2	

V-50: ballistic limit; P: partial penetration; C: complete penetration.

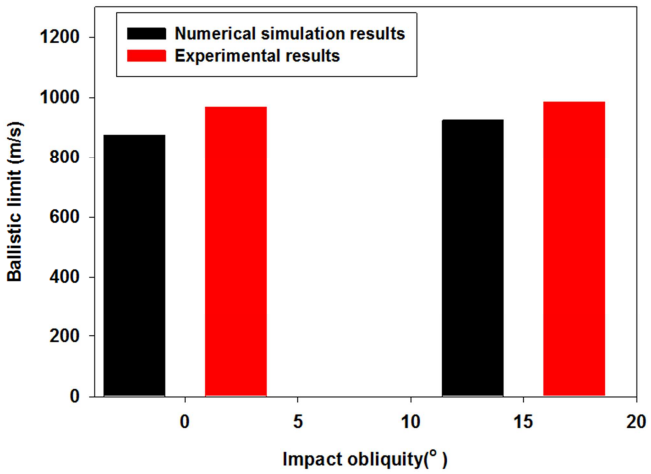

Fig. 6. Comparison of 3D numerical results with experimental results.

Figure 6 compares the simulation results in terms of the ballistic limits of TC-128 steel plate at different impact obliquities with the V-50 test data. It is shown that simulation results agree with experimental results quite well and the average error is about 8%. For both experimental and simulation results, the ballistic limit of TC -128 steel plates increased from 0º to 15º impact obliquity.

For obliquity impact, the projectile impacted the TC-128 steel plate with the side of the nose instead of the nose tip, which is equivalent to blunting the projectile tip. Compared with a sharp-nosed projectile, a blunt-nosed projectile needs more energy to perforate the same thickness target [18-20]. In addition, for obliquity impact, more target area will be affected, which is equivalent to increasing the target thickness. Both facts contributed to increasing the ballistic limit of the TC-128 steel plate under oblique impact. So, increasing the impact obliquity is a very effective way to protect the target, which will be discussed in the following section.

3. Vane Structure

A series of simulations are conducted here to study the effectiveness of a single-layer vane structure to protect theTC-128 steel plate. In order to save computational time, the length and width of TC-128 steel plate decreased from 300 mm × 300 mm to 200 mm × 200 mm since the affected zone of the TC-128 steel plate is only several times the size of the impact zone for high velocity impact. The other model constants for the projectile and TC-128 steel plate are the same as those in the previous part. The Lagrange solver is used for the vane structure. The total number of elements is 400, 800, and 1600 for the vane structure with thicknesses of 0.794, 1.588, 2.381 mm, respectively. The vane structure obliquity increased from 0º to 45º in steps of 15º. Two materials, aluminum and steel 1006, were used for the vane structure, respectively. The model constants of aluminum and steel 1006 are available in the AUTODYN library. EPS is chosen as the erosion criteria for both materials. The EPS values are 2.5 and 1 for aluminum and steel 1006, respectively. The length and width for all the vane structures are 200 mm × 200 mm. The architectures of single-layer aluminum and steel 1006 vane structures with a thickness 0.794 mm at different vane structure obliquities are shown in figure 7.

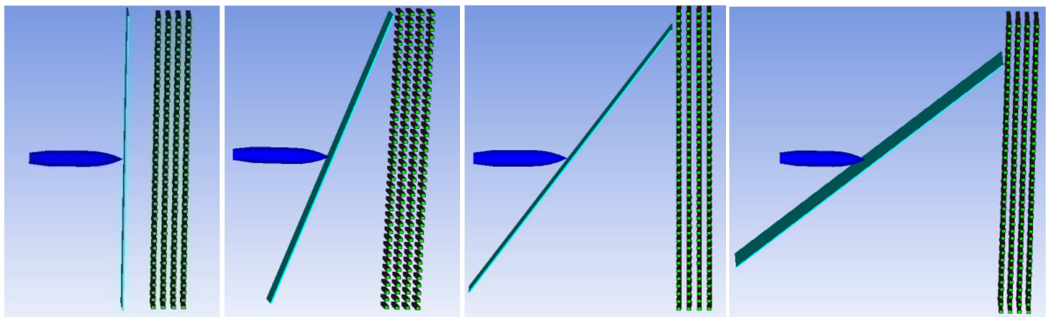

0º obliquity 15º obliquity 30º obliquity 45º obliquity

(a)

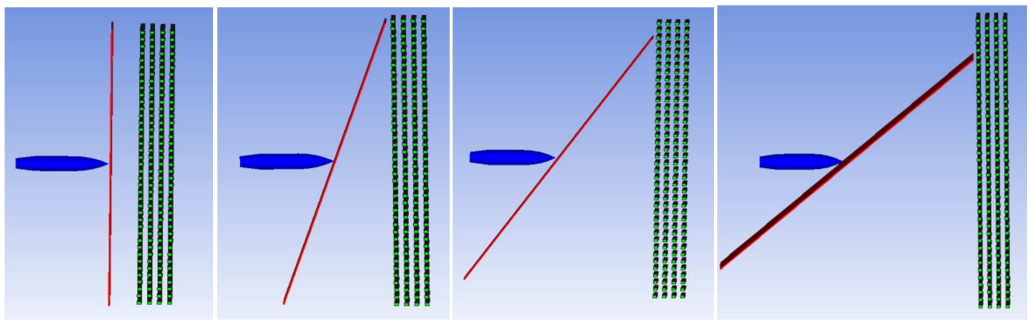

0º obliquity 15º obliquity 30º obliquity 45º obliquity

(b)

Fig. 7. Vane-target structure at different vane structure obliquities (a) Aluminum (b) Steel 1006.

The distribution density of the vane structure is also studied since it plays a very important role in increasing ballistic limit of vane- target structure. The single-layer aluminum vane structure with a thickness of 2.381 mm is used as a baseline. In order to keep areal density the same, a double-layer aluminum structure with a thickness of 1.191 mm for each layer vane is simulated in AUTODYN. The length and width for the layered vane structure are 200 mm x 200 mm. The horizontal distance between two vane structures is 50 mm. The architectures of the model for double-layer aluminum vane-targets are shown in figure 8.

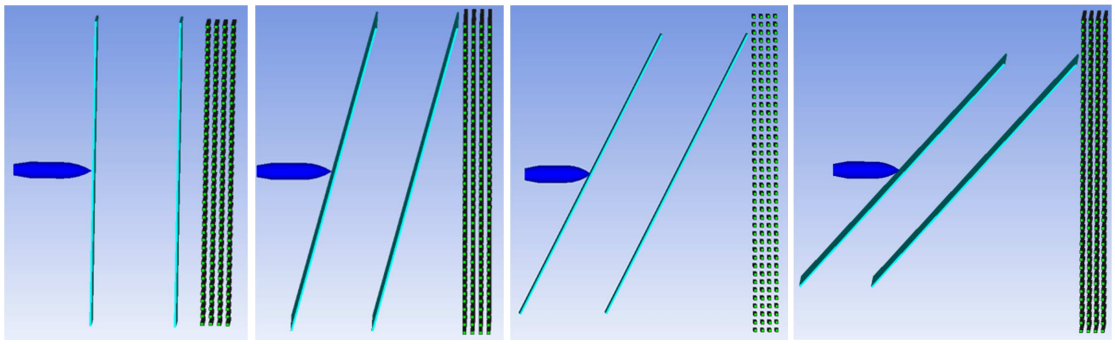

0º obliquity 15º obliquity 30º obliquity 45º obliquity

Fig. 8. Double layer aluminum vane-target structure at different vane structure obliquities.

4. Results and Discussions

The ballistic limit of single-layer aluminum and steel 1006 vane-target structures with different thicknesses and vane structure obliquities is reported in table 6. For both steel 1006 and aluminum vane structures, the ballistic limit increased with thickness and vane structure obliquity. The only exception is the 1.588, 2.381 mm steel 1006 vane structure at 45º obliquity. The reason is that the projectile impacted the TC-128 steel plate almost at 90º obliquity after the perforation of 1.588 mm steel 1006 vane structure at 45º obliquity. After perforation of the 2.381 mm steel 1006 vane structure at 45º obliquity, the projectile impacted TC-128 steel plate at angle less than 90º, which is illustrated in figure 9.

Table 6. Ballistic limit for single parallel aluminum and steel vane-target structure with different thicknesses and vane structure obliquities.

		Aluminum				Steel 1006			
Thickness (mm)	**Obliquity (Degree)**	**Impact velocity (m/s)**	**Result**	**Residual velocity (m/s)**	**V_{50} (m/s)**	**Impact velocity (m/s)**	**Result**	**Residual velocity (m/s)**	**V_{50} (m/s)**
0.794	0	910	p	0	920	1000	p	0	1010
		930	C	70.0		1020	C	30.0	
	15	1100	p	0	1110	1400	p	0	1410
		1120	C	110.3		1420	C	42.4	
	30	1190	p	0	1200	1500	p	0	1510
		1210	C	21.5		1520	C	43.7	
	45	1460	p	0	1470	1950	p	0	1955
		1480	C	54.0		1960	C	103.3	
1.588	0	1000	p	0	1005	1200	p	0	1210
		1010	C	51.0		1220	C	48.4	
	15	1130	p	0	1140	1420	p	0	1430
		1150	C	36.2		1440	C	42.8	
	30	1380	p	0	1390	1940	p	0	1950
		1400	C	56.8		1960	C	57.2	
	45	1600	p	0	1610	2480	p	0	2490
		1620	C	107.8		2500	C	172.2	
2.381	0	1010	p	0	1015	1300	p	0	1310
		1020	C	55.6		1320	C	269.9	
	15	1200	p	0	1210	1740	p	0	1750
		1220	C	68.3		1760	C	29.1	
	30	1500	p	0	1510	2200	p	0	2210
		1520	C	43.3		2220	C	64.9	
	45	1640	p	0	1650	2280	p	0	2290
		1660	C	38.1		2300	C	67.1	

V-50: Ballistic limit; P: Partial penetration; C: Complete penetration.

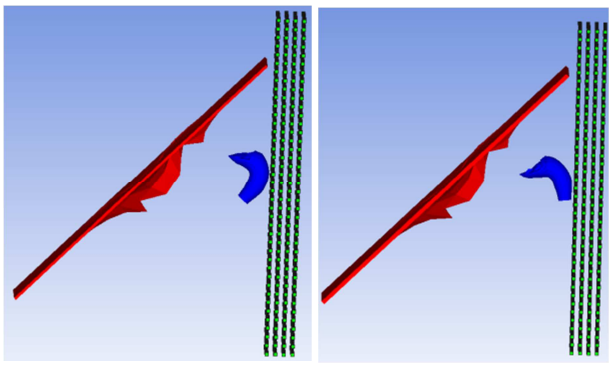

(a) (b)

Fig. 9. Projectile impact TC-128 steel plate after perforation of different thickness steel 1006 vane structures at 45º obliquity (a) 1.588 mm (b) 2.381 mm.

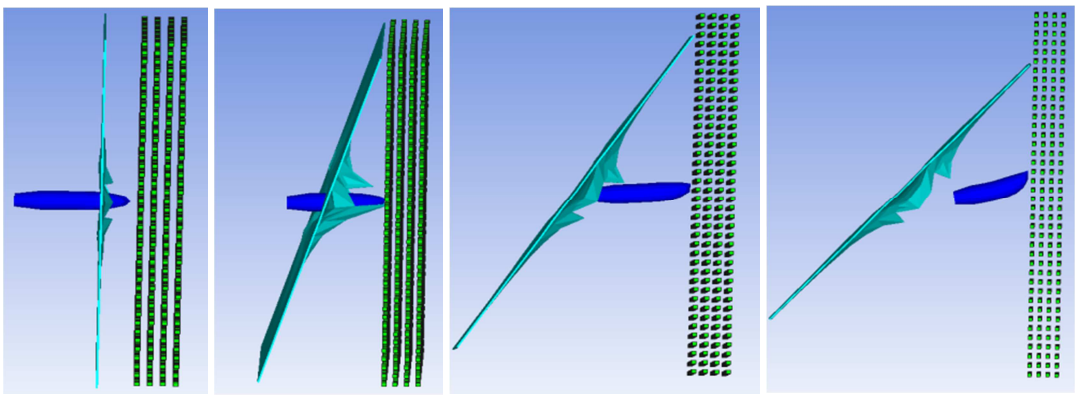

0º obliquity 15º obliquity 30º obliquity 45º obliquity

(a)

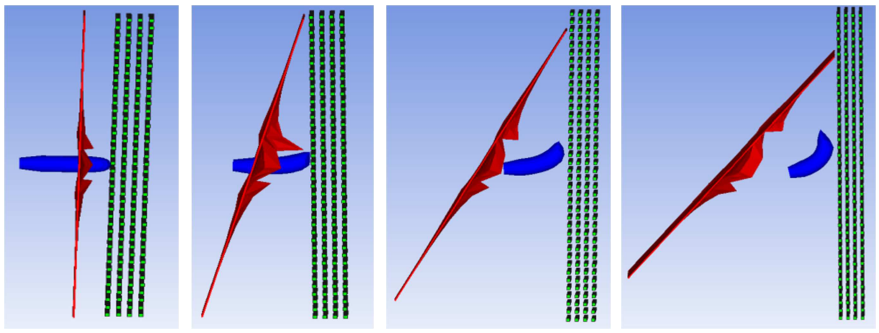

0º obliquity 15º obliquity 30º obliquity 45º obliquity

(b)

Fig. 10. Deflection of projectile impact against 0.794 mm thick vane structure at different vane structure obliquities (a) Aluminum (b) Steel 1006

Figure 10 depicts the deflection of the projectile after perforation of the 0.794 mm single-layer aluminum and steel 1006 vane structures with different vane structure obliquities. The deflection of the projectile increased with vane structure obliquity for both aluminum and steel 1006 vane structures. For the same vane structure obliquity, the steel 1006 vane structure can deflect the projectile more than the aluminum vane structure because of the higher strength of steel 1006. The deflection of the projectile will lead to projectile impact on the target structure in certain angle, which will increase the ballistic limit of vane-target structure [21, 22] .

Figure 11 compares the ballistic limit of single-layer aluminum and steel 1006 vane-target structures. The ballistic limit of the steel 1006 vane-target structure is much higher than that of the aluminum target structure with the same thickness and obliquity. This is due to the fact that more energy is needed to perforate the steel 1006 vane structure than the aluminum vane structure at the same thickness. More importantly, compared with the aluminum vane structure, the steel 1006 vane structure with the same thickness will lead to the impact of the projectile on the TC-128 steel plate at a higher obliquity, which is also shown in figure 10.

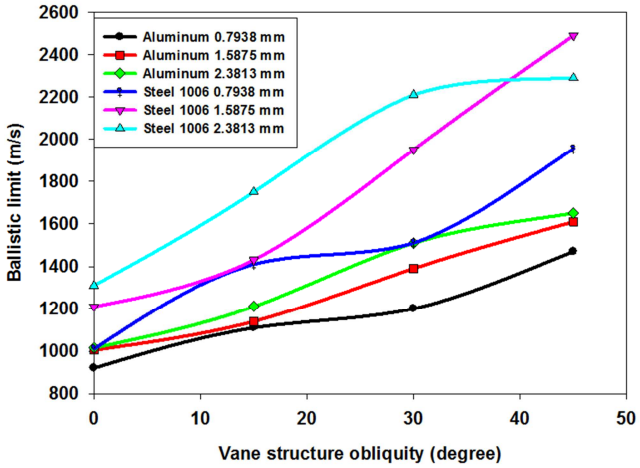

Fig. 11. Ballistic limit of single-layer aluminum and steel 1006 vane structures at different thicknesses and vane structure obliquities.

Increased ballistic performance is always accompanied by an increase in material weight. It is necessary to compare the improvement in the ballistic performance of TC-128 steel plate because of aluminum and steel vane structure at unit areal density. The vane structure's "Vane Isolated Performance" (VIP) can be described as,

$$V\text{-}50_{VIP}=(V\text{-}50_{vane+target}-V\text{-}50_{vane})/\text{areal density of vane structure} \quad (4)$$

Table 7. "Vane Isolated Performance" (VIP) of aluminum and steel 1006 vane structures.

			Aluminum			Steel 1006		
Thickness (mm)	**Obliquity (Degree)**	**Target v-50 (m/s)**	**Vane + Target V-50 (m/s)**	**Areal density (kg/m^2)**	**VIP (m/s)/ (kg/m^2)**	**Vane + target V-50 (m/s)**	**Areal density (kg/m^2)**	**VIP (m/s)/ (kg/m^2)**
0.794	0	875	920	2.15	20.9	1010	6.27	21.5
	15	875	1110		109.2	1410		85.4
	30	875	1200		151.1	1510		101.3
	45	875	1470		276.6	1955		172.3
1.588	0	875	1005	4.30	30.2	1210	12.53	26.7
	15	875	1140		61.6	1430		44.3
	30	875	1390		119.7	1950		85.8
	45	875	1610		170.8	2490		128.8
2.381	0	875	1015	6.45	21.7	1310	18.80	23.1
	15	875	1210		51.9	1750		46.5
	30	875	1510		98.4	2210		71.0
	45	875	1650		120.1	2290		75.3

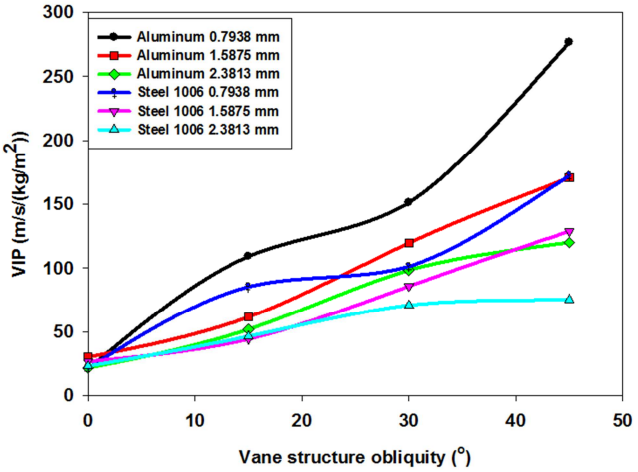

Fig. 12. VIP of aluminum and steel 1006 vane structures at different thicknesses and vane structure obliquities.

The VIP of single-layer aluminum and steel 1006 vanes at different vane structure obliquities are presented in table 7 and figure 12. For both single-layer aluminum and steel vane structures, the VIP increased with increasing vane structure obliquity and decreased with increasing thickness of vane structure. The VIP of the aluminum vane structure is higher than that of the steel 1006 vane structure at the same thickness and vane structure obliquity because of the lower areal density of aluminum. So, lightweight but high-strength materials are perfect for the vane structure.

The ballistic limit of layering steel vane-target structure is tabulated in table 8. With the same areal density, the double-layer vane structure has the better ballistic performance. The VIP of the layered vane-target structure is also reported in table 8 and figure 13. It is shown that the single-layer vane structure has a lower VIP than the double-layer vane structure. Figure 14 shows the deflection of the projectile after perforation of the single- and double-layer aluminum vane structures. With the same vane structure obliquity, the double vane structure can deflected the projectile more than the single-layer vane structure, which will result in the impact of the projectile on the TC 128 steel plate at a higher obliquity. This is the reason why the double-layer vane structure is a more efficient structure for ballistic performance.

Table 8. "Vane Isolated Performance" (VIP) of single and double layer aluminum vane structure.

		Single layer			Double layer		
Obliquity (Degree)	**Target v-50 (m/s)**	**Vane+target V-50 (m/s)**	**Areal density (kg/m²)**	**VIP (m/s)/(kg/m²)**	**Vane+target V-50 (m/s)**	**Areal density (kg/m²)**	**VIP (m/s)/ (kg/m²)**
0	875	1015	6.27	21.7	1030	6.27	24.0
15	875	1210		51.9	1290		64.3
30	875	1510		98.4	1620		115.4
45	875	1650		120.1	1990		172.8

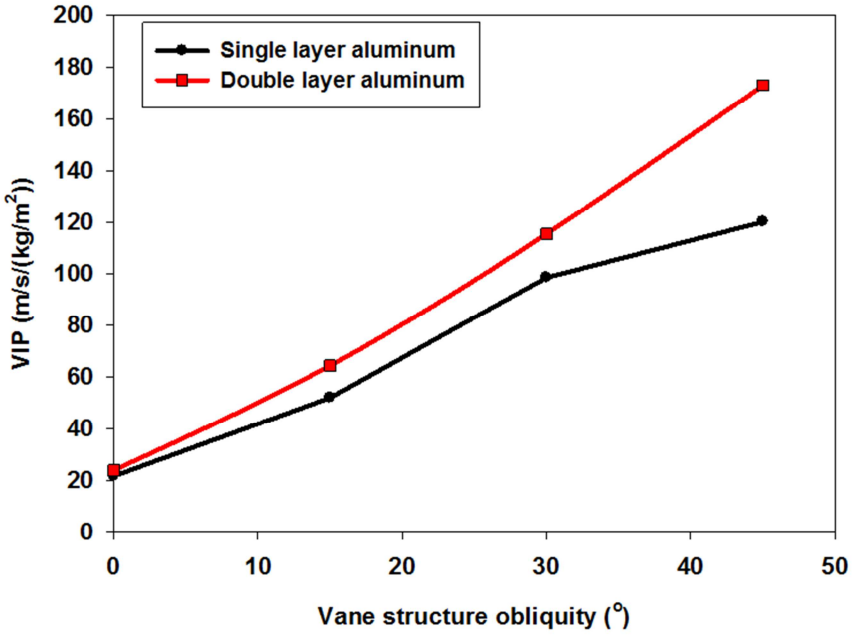

Fig. 13. VIP of single- and double-layer aluminum vane structures at different vane structure obliquities.

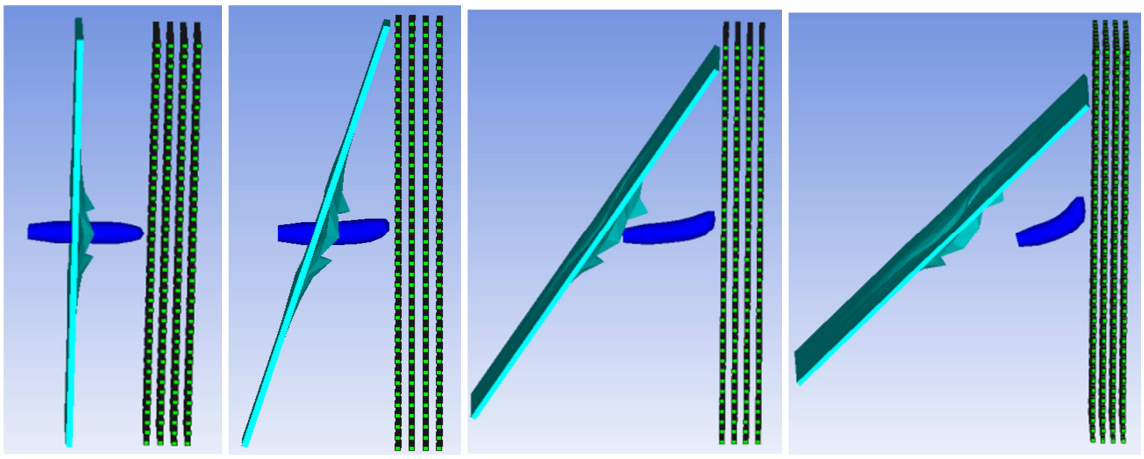

Fig. 14. Deflection of projectile due to aluminum vane structure at different vane structure obliquities (a) single-layer (b) double-layer.

5. Conclusions

V-50 tests have been carried out for TC-128 steel plate impact by 0.50 caliber M33 ball round projectile at 0º, 15º, 30º and 45º obliquity. Three-dimensional numerical simulations have been conducted to study the ballistic performance of the TC-128 steel plate under normal and oblique impact. Three-dimensional numerical simulations also have been performed to investigate the "Vane Isolated Performance" of aluminum and steel 1006 vane-target structures at different vane structure obliquities. Based on experimental and numerical results, main conclusions can be drawn as follows:

1 The simulation results agree with experimental results well, and the average error is about 8%. For both experimental and simulation results, the ballistic limit of TC-128 steel plates increased from 0º to 15º impact obliquity.

2 The vane structure can effectively protect the TC-128 steel plate. For single-layer aluminum and steel 1006 vane structures, the ballistic limit of the vane-target structure increased with vane structure obliquity and thickness. Compared with aluminum vane-target structures, the steel 1006 vane-target structure has a higher ballistic limit due to higher strength.

3 For both single-layer aluminum and steel 1006 vane structures, the "Vane Isolated Performance" increases with increasing vane structure obliquity and decreases with increasing thickness of vane structure.

4 For the same thickness of vane structure, the VIP of aluminum vane structures is higher than that of steel 1006 vane structures because of the lower areal density of aluminum. So, the lightweight but high strength material can optimize the vane structure.

5 The double-layer structure provides more VIP than the single-layer vane structure. So the double-layer vane structure is a more efficient structure for ballistic performance.

Acknowledgements

Authors acknowledge the financial support received under a subcontract from the Department of Homeland Security-sponsored Southeast Region Research Initiative (SERRI) at the Department of Energy's Oak Ridge National Laboratory for this research work.

References

[1] B.J.M. Ale, G. Golbach, D. Goos, K. Ham, L. Janssen, S. Shield, Benchmark risk analysis models. RIVM Report 610066015. (2001) 1-48.

[2] S.R. Hanna, O.R. Hansen, M. Ichard, D. Strimaitis, CFD model simulation of dispersion from chlorine railcar releases in industrial and urban areas, Atmospheric Environment, 43 (2009) 262-270.

[3] M.R. Saat, C.P.L. Barkan, The Effect of Rerouting and Tank Car Safety Design on the Risk of Rail Transport of Hazardous Materials, 7th World Congress on Railway research, (2006).

[4] M.C. Fowler, Experimental and numerical analysis of nano-enhanced polymer coated steel plates subjected to ballistic loading, in, Thesis, The University of Mississippi, 2012.

[5] S. Sadanandan, J.G. Hetherington, Characterisation of ceramic/steel and ceramic/aluminium armours subjected to oblique impact, International Journal of Impact Engineering, 19 (1997) 811-819.

[6] R.B. Bogoslovov, C.M. Roland, R.M. Gamache, Impact-induced glass transition in elastomeric coatings, Applied Physics Letters, 90 (2007) 221910.

[7] S.S. Sarva, S. Deschanel, M.C. Boyce, W. Chen, Stress–strain behavior of a polyurea and a polyurethane from low to high strain rates, Polymer, 48 (2007) 2208-2213.

[8] C.M. Roland, D. Fragiadakis, R.M. Gamache, Elastomer–steel laminate armor, Composite Structures, 92 (2010) 1059-1064.

[9] M. Grujicic, B. Pandurangan, T. He, B.A. Cheeseman, C.F. Yen, C.L. Randow, Computational investigation of impact energy absorption capability of polyurea coatings via deformation-induced glass transition, Materials Science and Engineering: A, 527 (2010) 7741-7751.

[10] G. Sundararajan, The energy absorbed during the oblique impact of a hard ball against ductile target materials, International Journal of Impact Engineering, 9 (1990) 343-358.

[11] M.A. Iqbal, A. Chakrabarti, S. Beniwal, N.K. Gupta, 3D numerical simulations of sharp nosed projectile impact on ductile targets, International Journal of Impact Engineering, 37 (2010) 185-195.

[12] T. Børvik, L. Olovsson, S. Dey, M. Langseth, Normal and oblique impact of small arms bullets on AA6082-T4 aluminium protective plates, International Journal of Impact Engineering, 38 (2011) 577-589.

[13] A.H. Baluch, Y. Park, C.G. Kim, High velocity impact characterization of Al alloys for oblique impacts. Acta Astronautica. 105 (2014) 128-135.

[14] M.N. Roslan, A.E. Isrnail, M.Y. Hashim, M.H. Zainulabidin, S.N.A. Khalid, Modelling analysis on mechanical damage of kenaf reinforced composite plates under oblique impact loadings. Applied Mechanics and Materials. 465-466 (2013) 1324-1328.

[15] T. Børvik, S. Dey, A.H. Clausen, Perforation resistance of five different high-strength steel plates subjected to small-arms projectiles, International Journal of Impact Engineering, 36 (2009) 948-964.

[16] T. Børvik, O.S. Hopperstad, T. Berstad, M. Langseth, A computational model of viscoplasticity and ductile damage for impact and penetration, European Journal of Mechanics - A/Solids, 20 (2001) 685-712.

[17] S. Dey, T. Børvik, O.S. Hopperstad, J.R. Leinum, M. Langseth, The effect of target strength on the perforation of steel plates using three different projectile nose shapes, International Journal of Impact Engineering, 30 (2004) 1005-1038.

[18] T. Børvik, M. Langseth, O.S. Hopperstad, K.A. Malo, Perforation of 12 mm thick steel plates by 20 mm diameter projectiles with flat, hemispherical and conical noses: Part I: Experimental study, International Journal of Impact Engineering, 27 (2002) 19-35.

[19] T. Børvik, O.S. Hopperstad, T. Berstad, M. Langseth, Perforation of 12 mm thick steel plates by 20 mm diameter projectiles with flat, hemispherical and conical noses: Part II: numerical simulations, International Journal of Impact Engineering, 27 (2002) 37-64.

[20] N.K. Gupta, M.A. Iqbal, G.S. Sekhon, Effect of projectile nose shape, impact velocity and target thickness on the deformation behavior of layered plates, International Journal of Impact Engineering, 35 (2008) 37-60.

[21] Z. Fawaz, W. Zheng, K. Behdinan, Numerical simulation of normal and oblique ballistic impact on ceramic composite armours, Composite Structures, 63 (2004) 387-395.

[22] N.K. Gupta, V. Madhu, Normal and oblique impact of a kinetic energy projectile on mild steel plates, International Journal of Impact Engineering, 12 (1992) 333-343.